Radiated Emission Modeling of a Wireless Power Transfer System

Hanyu Zhang^{#1}, Guanghua Li^{*2}, Viswa Pilla^{*3}, and Chulsoon Hwang^{#4}

*EMC Laboratory, Missouri University of Science and Technology, Rolla, MO, USA

*Apple Inc., Cupertino, California, USA

¹hzc5z, ⁴hwangc@mst.edu, ²guanghua li, ³viplla@apple.com

Abstract—A radiated emission (RE) model of a wireless power transfer (WPT) system is proposed in this paper to help designers predict, analyze, and mitigate the RE issues during the design process. The proposed model employs both full-wave simulation and circuit simulation to derive a transfer function. Subsequently, it predicts the emission level by combining the transfer function with the measured transmitter waveform through a straightforward calculation. The predicted emissions match the measured RE peaks well up to 300 MHz, with the error within 3 dB. The impact of functional parameters, such as load and coil gap distance, is analyzed based on the proposed model

Keywords—Electromagnetic interference, emission modeling, radiated emission, wireless power transfer

I. INTRODUCTION

Wireless power transfer (WPT) technology enables the transfer of energy without the need for physical connectors, providing enhanced convenience and flexibility in charging electronic devices, and has been widely used in various applications. However, the electromagnetic fields generated during the wireless power transfer process pose challenges in terms of electromagnetic interference (EMI).

WPT systems use power semiconductor switches to drive transmitting coils, the switches generate strong noise during the turn-on and turn-off transients, eventually causing EMI problems. EMI contains conducted emission (CE) at lower frequencies (below 30 MHz) and radiated emission (RE) at higher frequencies (above 30 MHz). RE is an important factor to consider when designing a WPT system. However, directly measuring RE from a WPT system is time- and effort-consuming necessitating a semi-anechoic chamber, spectrum analyzer, and receiving antenna [1]. Consequently, there is a need for a straightforward method to predict RE in WPT systems.

While extensive research has been conducted on EMI in power converters [2]-[5], there is a limited body of literature specifically addressing EMI in WPT systems. In [6], it is found that, depending on the source type, the RE of a multicoil WPT system increases at the series or parallel resonance peaks. In [7], the CM current in a WPT system was analyzed, and then the CE of a Qi-compliant WPT system was predicted up to 30 MHz. In [8], the RE of a WPT system from 30 MHz to 1 GHz was investigated, the authors found that the RE is caused by the CM current in the USB cables, and the transmitter is the noise source for the emission, however, the RE model neglected the effects of the coil and cannot be readily generalized. Although these methods provide a good understanding of the EMI of a WPT system, there is still no simple and reliable method to predict the RE of a WPT system.

This paper analyzes the radiation mechanism of a WPT system and introduces a RE model, capable of predicting RE up to 300 MHz. The model divides RE estimation into two parts: source and transfer function. The paper outlines the

procedure for extracting the transfer function. Additionally, the influence of load, coil gap distance, and matching capacitors on the RE of the WPT system is analyzed.

II. RADIATION EMISSION MODEL

A. Wireless Power Transfer System

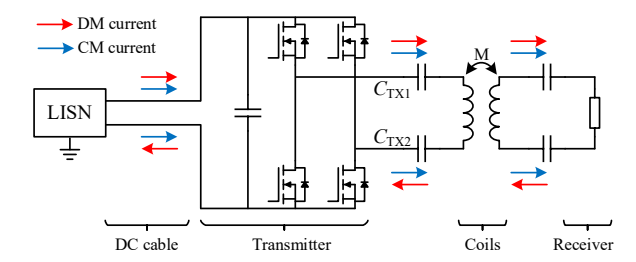


Fig. 1. Block diagram of WPT system.

This study employs a mock-up WPT system, featuring a transmitter, coupling coils, and a receiver, as depicted in Fig. 1. The transmitter is powered by a 15-V DC power supply connected through a cable to a line impedance stabilization network (LISN). Operating with a square waveform, the transmitter drives the transmitting coil via the matching capacitors. A voltage induced across the receiving coil is picked up by the receiver with matching capacitors. Finally, the received power is dissipated through the load resistor.

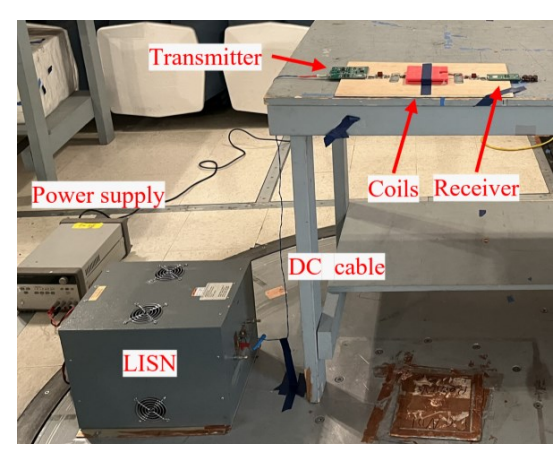


Fig. 2. A picture of the mock-up WPT system.

In Fig. 2, a picture of the WPT system under the test is presented. The system was tested in a 3-meter semi-anechoic chamber. The WPT system was positioned on a table, elevated 0.9 meters above the ground, while the LISN was situated on the ground. This configuration required the DC cable to ascend to the transmitter. The coupling coils were securely affixed to a 3D-printed fixture, allowing for straightforward control of the alignment conditions.

B. Radiated Emission Mechanism

The transmitter employs a full bridge circuit to generate a square waveform. With two output terminals, each producing a square waveform with a 50% duty cycle, the high level equals the input voltage, and the low level is 0 V, as shown in Fig. 3(a). The phase difference between the two terminals is 180°. The transmitting coil is driven by the differential mode voltage between the terminals. Energy is wirelessly transferred from the transmitting coil to the receiving coil via inductive coupling. However, the transmitter output contains common mode components. In Fig. 3(b), the common mode voltage spectrum of the transmitter output is depicted. The spectrum consists of harmonic peaks. For clarity in subsequent figures throughout this paper, only the upper envelope of spectrums will be displayed.

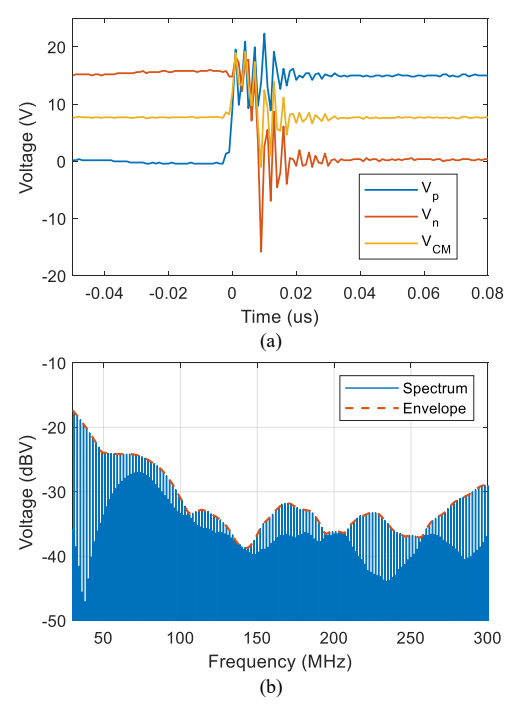


Fig. 3. (a) Waveform and (b) spectrum of the transmitter CM output voltage.

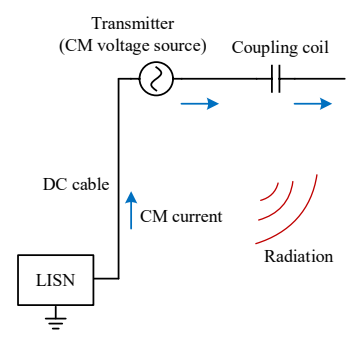


Fig. 4. CM current path in the WPT system responsible for RE.

The coupled coils are part of the common mode current path. Specifically, in our scenario, the receiving coil was positioned a few millimeters above the transmitting coil. The CM current flows from the transmitting coil to the receiving coil through capacitive coupling. Therefore, the coupling coil can be represented a lumped capacitor within the context of the CM

current path. The CM output of the transmitter drives the DC input cable against the rest of the system, inducing CM current in the system, as depicted in Fig. 4. The impact of the received RE level can be divided into source and path as

$$V_{RE}(f) = V_{CM}(f) \times TF(f) , \qquad (1)$$

where V_{RE} is the received voltage of the receiving antenna representing the RE strength at the antenna location, the antenna voltage can be converted to an electric field by multiplying it with the antenna factor, $V_{\rm CM}$ is the CM voltage of the transmitter output, which is also the source of the radiation, TF is a transfer function defined as the ratio of RE to the transmitter CM output voltage, representing the coupling from source to receiving antenna.

C. Radiated Emission Modeling

To predict the coupling to the receiving antenna, a full-wave simulation model was constructed in the CST. The simulation model, depicted in Fig. 5, encompasses the LISN, input DC cable, transmitter, coils, and receiver. As RE stems from the CM current within the system, the simulation modeled only the CM current path.

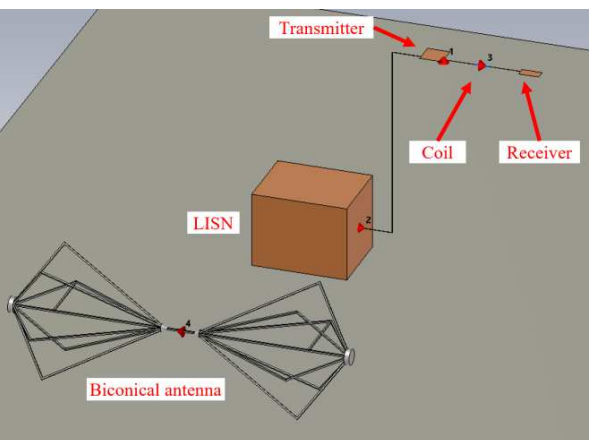


Fig. 5. Full-wave simulation model in CST.

In the actual WPT system, the transmitter and receiver are implemented on printed circuit boards (PCB), but they are simplified as copper sheets in the simulation. In the transmitter, the input cable is directly connected to the copper sheet, and the output wire to the coil is connected to the sheet through an S-parameter port representing the transmitter output (see Fig. 5). The receiving coil is connected to the receiver via a cable. Cables having both positive wire and negative wire are treated as single wires as the CM current in these cables is identical. The matching capacitors, situated in the cables, are in the nano-Farad range. Their impedance is small enough to be ignored for the frequency range of interest.

The coil is represented as a port symbolizing its CM impedance. The LISN is modeled as a metallic box, with the input DC wire connected to the LISN through a port symbolizing the CM input impedance of the LISN. In the actual measurement, a biconical antenna captured the RE. For an accurate simulation of the received emission level, this biconical antenna was modeled, with its output connected to a port to measure the antenna output voltage. The outcome of the full-wave simulation is 4-port S-parameters that describe the relationship among CM voltage sources (port 1), LISN

CM impedance (port 2), coil CM impedance (port 3), and the biconical antenna output (port 4).

The CM impedance of the LISN was measured using a vector network analyzer (VNA), as illustrated in Fig. 6(a). During this measurement, the positive and negative terminals were shorted using a wire denoted as connection wire in Fig. 6 (a). The LISN CM impedance is defined as the impedance between the connection wire and the LISN metallic case. The measurement result is depicted in Fig. 6(b). The nominal LISN CM impedance is 25 Ω . However, the measurement result indicates that the LISN CM impedance is larger than 25 Ω when frequency is higher than 150 MHz. It is imperative to use the measured impedance in predicting RE up to 300 MHz.

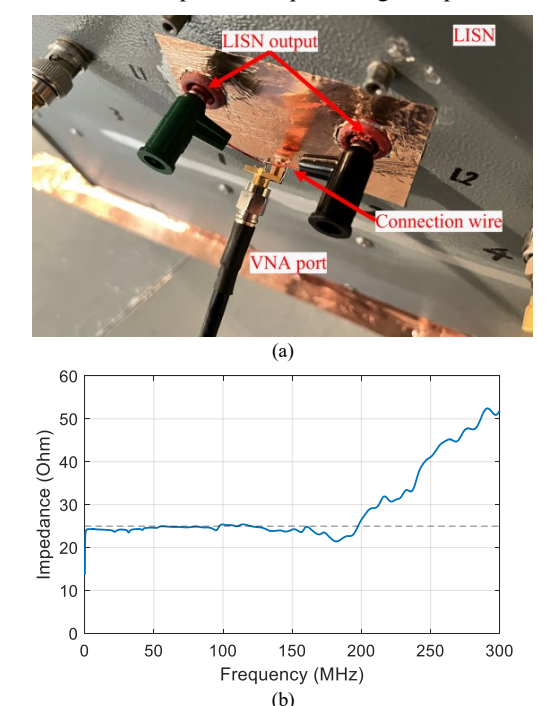


Fig. 6. LISN CM impedance (a) measurement setup and (b) measurement

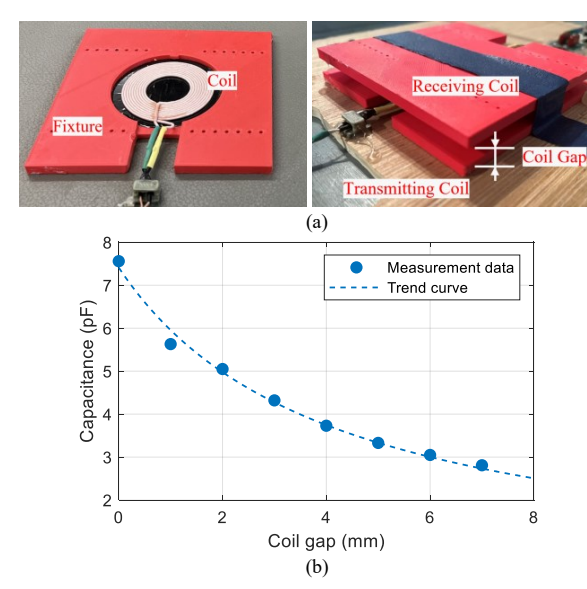


Fig. 7. (a) Pictures and (b) CM capcitance of the coupling coil.

The CM current flows from the transmitting coil to the receiving coil capacitively, leading to the modeling of the coupling coil as a lumped capacitor concerning its CM behavior. The transmitting coil and receiving coil were fixed in the fixture as shown in Fig. 7(a), with the coil gap distance defined from the top surface of the transmitting coil to the bottom surface of the receiving coil. For the measurement of coil CM capacitance, the two terminals of the transmitting coil, as well as the receiving coil, need to be shorted. The coil capacitance is determined as the capacitance between the two connection points. Subsequently, the coil capacitance value was measured by an LCR meter. Fig. 7 (b) shows the measurement results of the coil capacitance at various gap distances. As expected, as the gap distance increases, the coil capacitance decreases, resembling the behavior of a parallel plate capacitor. The coil capacitance is in the pico-Farad range, exhibiting an impedance of tens to thousands of ohms in the frequency of interest, and cannot be ignored in the RE model.

To predict the RE level, a circuit simulation model, as shown in Fig. 8, was built in ADS. In this model, the full-wave simulation result was imported as a 4-port S-parameter block (SnP1). The ports in Fig. 8 correspond to ports in Fig. 5. The measured LISN CM impedance was imported as a 1-port Sparameter block (SnP2). The transmitter CM output was modeled as a voltage source (SRC3). C1 represents the coupling coil CM capacitance. R1 represents the load impedance of the biconical antenna. The output impedance of the biconical antenna impedance is 200 Ω . For impedance matching, in the actual measurement, the biconical antenna was connected to a spectrum analyzer (50 Ω input impedance) through a 4:1 balun. Considering the input and output relationship of the 4:1 balun, 6 dB is subtracted to the simulated voltage level at the biconical antenna output to compensate for the balun effect. By performing the circuit simulation in the frequency domain, the ratio of RE level to transmitter CM output can be found, which is the transfer function defined in (1).

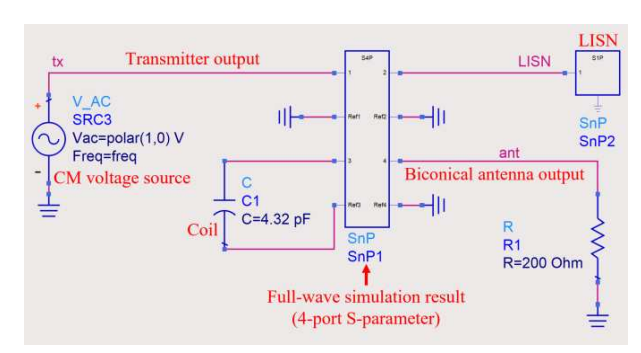


Fig. 8. Circuit simulation model for the RE transfer function.

To extract the transmitter CM output voltage, the positive terminal output voltage $V_p(t)$ and negative terminal output voltage $V_n(t)$ should be measured simultaneously. The CM output voltage waveform $V_{\text{CM}}(t)$ is calculated by (2)

$$V_{\rm CM}(t) = \frac{V_{\rm p}(t) + V_{\rm n}(t)}{2} \,. \tag{2}$$

The CM output voltage is then converted to the frequency domain by fast Fourier transform (FFT):

$$V_{\text{CM}}(f) = \text{FFT} \left[V_{\text{CM}}(t) \right].$$
 (3)

Using (1) and (3), the RE level in the frequency domain can be calculated. It needs to be noted that the voltage waveform $V_p(t)$ and $V_n(t)$ are from measurement, and the transfer function TF(f) is from simulation.

III. PARAMETERIC ANALYSIS

A. Load Resistance

The RE from a WPT system is load-dependent, therefore, the mock-up WPT system was tested with 9-ohm, 20-ohm, and 56-ohm loads respectively. Then the proposed RE prediction method was performed for all cases.

Fig. 9 is the upper envelope of the measured transmitter CM output voltage spectrum under different load conditions, the result indicates the transmitter output voltage is load dependent, the transmitter CM output voltage decreases with the increase of load resistance.

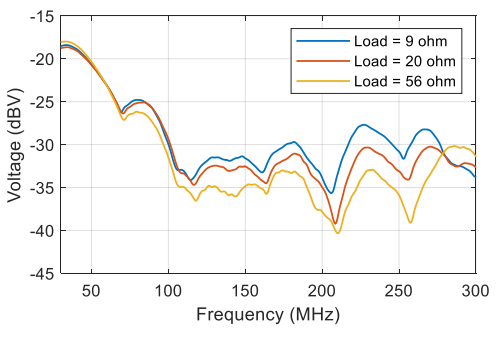


Fig. 9. Upper envelope of the measured transmitter CM output voltage spectrum under different load conditions.

The transfer function is determined by the system geometry structure, the LISN impedance, and the coil capacitance which remain the same when the load resistance changes, so the transfer function is load independent. Fig. 10 shows the RE transfer functions simulation result for both horizontal and vertical polarizations.

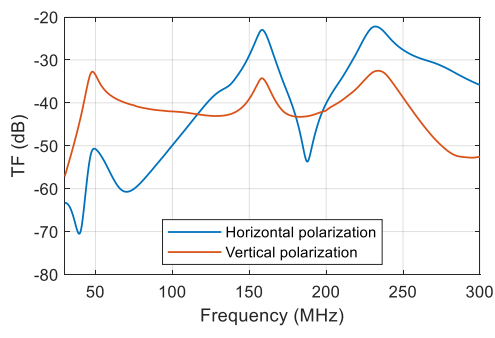


Fig. 10. RE Transfer functions for both horizontal polarization and vertical polarization.

Combining the transmitter CM output voltage spectrum and simulated transfer functions by (1), the RE of the WPT system under different load conditions can be predicted. The comparison between predicted and measured RE levels is shown in Fig. 11. The predicted RE trend matches the measurement result well, the amplitude error of the predicted RE peak is within 3dB. Based on the RE prediction procedure, the difference in the RE under different load conditions is because the transmitter output changes with the load.

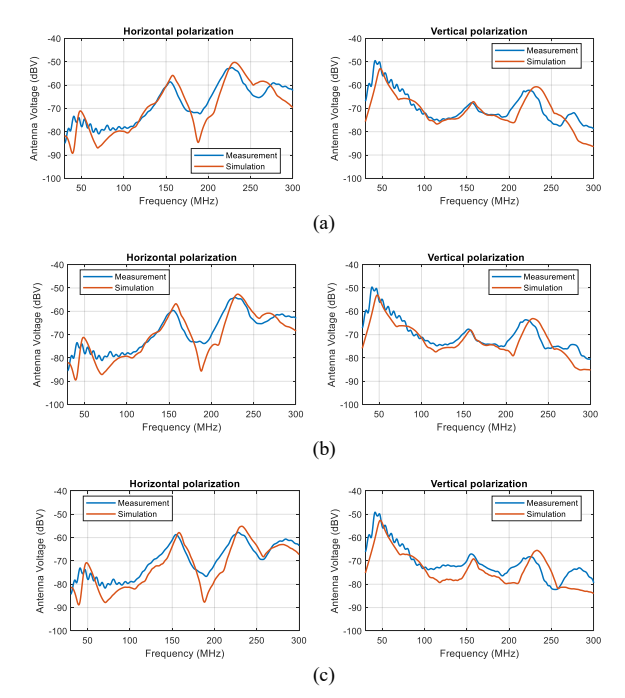


Fig. 11. Comparison of measured and predicted RE level under (a) 9-ohm, (b) 20-ohm, and (c) 56-ohm load conditions.

B. Coil Gap Distance

A WPT system is supposed to work with different coil gap distances, so the mock-up WPT system was tested with coil gap distances of 1 mm, 3 mm, and 5 mm. The transmitter output voltage under different coil gap distances was measured, Fig. 12 shows the measurement result, the cases with 3 mm and 5 mm coil gaps show similar spectrum levels, the difference is within 2 dB, meanwhile, the spectrum of the 1 mm coil gap case is much lower.

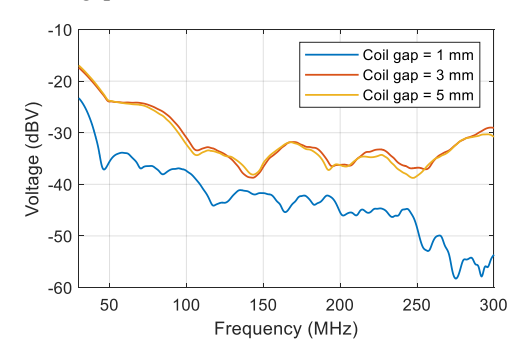


Fig. 12. Upper envelope of the transmitter CM output voltage spectrum with different coil gap distances.

The coil CM capacitance changes with the coil gap distance as shown in Fig. 7(b). The RE transfer functions of different coil gap distances were extracted by updating the coil capacitance in the circuit simulation in Fig. 8, and the result is shown in Fig. 13. The result indicates that the transfer function depends on the coil gap distance, and both the amplitude and peak frequency of the transfer function change when the coil gap distance changes.

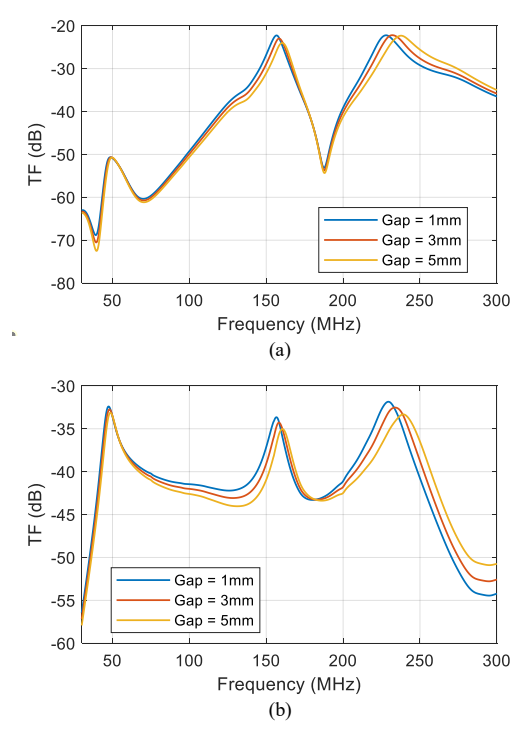


Fig. 13. RE transfer functions with different coil gap distances for (a) horizontal polarization and (b) vertical polarization.

Multiplying the source voltage spectrum in Fig. 12 and the RE transfer function in Fig. 13, the RE results with different coil gap distances were predicted, which are shown in Fig. 14. The predicted result matches the measurement data, with the error within 3dB for the RE peaks, except for the peak at 40 MHz in vertical polarization.

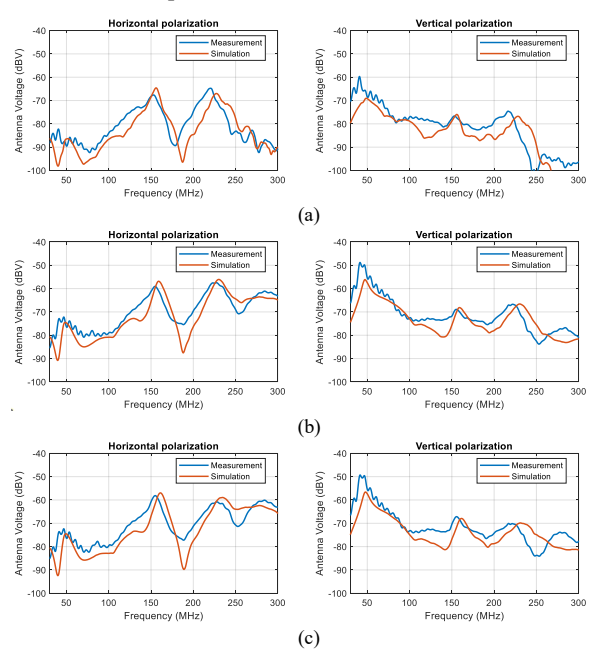


Fig. 14. Comparison of measured and predicted RE level when the coil gap is (a) 1 mm, (b) 3 mm, and (c) 5 mm.

Although the RE transfer function of the 1 mm case is a few decibels higher than others, the 1 mm case still has the lowest RE level since its source is much lower than others.

C. Matching Capacitor

The mock-up WPT system has two transmitting matching capacitors $C_{\rm TX1}$ and $C_{\rm TX2}$ as shown in Fig. 1. Both the transmitting matching capacitors were 4.7 nF, and then were replaced with 6.9 nF capacitors to test the RE. Changing the matching capacitors doesn't change the RE transfer function, instead, it changes the CM source because the load impedance of the transmitter changes. Fig. 15 shows the spectrum of the transmitter CM output voltage. The case using 6.9 nF transmitting matching capacitors has a lower CM voltage spectrum level.

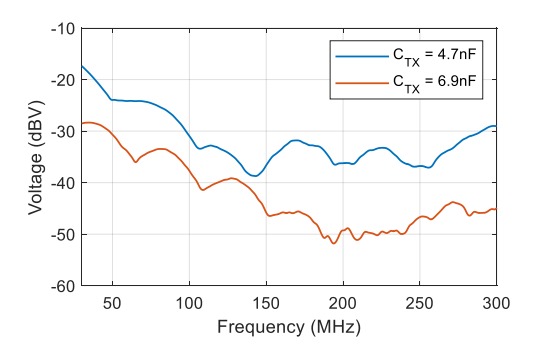


Fig. 15. Upper envelope of the transmitter CM output voltage spectrum with different transmitting matching capaictors.

The RE prediction result was obtained by applying the RE prediction method, and the comparison between the measured RE and prediction result is shown in Fig. 16. The comparison indicates that the case with 6.9 nF transmitting matching capacitors has a lower RE level due to the lower source voltage. The predicted RE shows a good correlation with the measurement result.

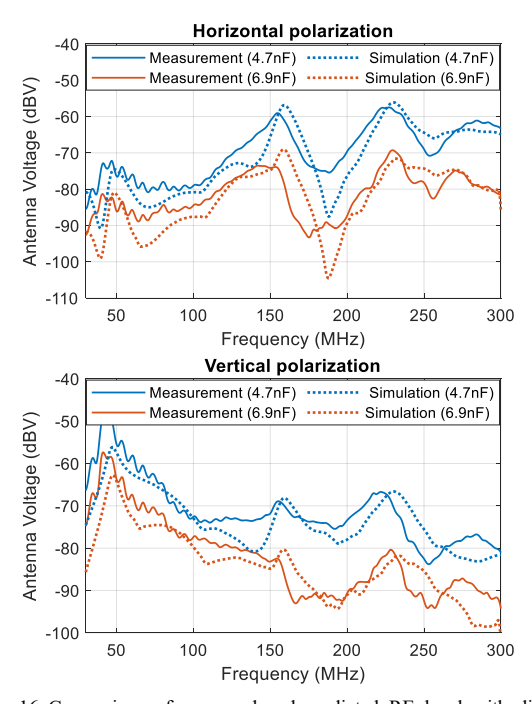


Fig. 16. Comparison of measured and predicted RE level with different transmitting matching capacitors.

D. Discussion

From the successful validation of the proposed model, the impact of the functional parameters on the RE can be divided into two parts: source and path. The source is quantified by the CM voltage spectrum, and the path is quantified by a RE transfer function. When analyzing a functional parameter, the source spectrum and RE transfer function can be compared between different parameter values, then the contribution of the source and path can be easily distinguished so that the designer can optimize the design accordingly. In this paper, the impact of the load resistance, coil gap distance, and matching capacitors are analyzed. However, the functional parameter is not limited to these, other parameters like cable length and cable arrangement can also be analyzed with the proposed method.

IV. CONCLUSION

In this paper, a WPT system RE prediction method is proposed. This method divides the RE into two parts: source and path. The source is the transmitter output, and the path is quantified by a transfer function that is obtained in conjunction with a full-wave simulation and a circuit simulation. The RE is predicted by multiplying the source voltage spectrum and the transfer function. The proposed method is validated up to 300 MHz by comparing the predicted and measured RE. The proposed method can be used to analyze the impact of functional parameters of a WPT system on RE.

REFERENCES

 Z. Sun, X. Wang, C. Wu, B. Kim, D. Kim and J. Fan, "Estimating Electromagnetic Emissions from a Site Installation with Multiple Racks of Server Equipment," in 2021 IEEE International Joint

- EMC/SI/PI and EMC Europe Symposium, Raleigh, NC, USA, 2021, pp. 1058-1063.
- [2] Y. Zhang, S. Wang and Y. Chu, "Investigation of Radiated Electromagnetic Interference for an Isolated High-Frequency DC–DC Power Converter With Power Cables," *IEEE Transactions on Power Electronics*, vol. 34, no. 10, pp. 9632-9643, Oct. 2019.
- [3] Z. Ma et al., "Radiated EMI Prediction in Power Converters with Power Cables Based on Cable Antenna Voltage Gain Extraction," in 2022 IEEE International Symposium on Electromagnetic Compatibility & Signal/Power Integrity (EMCSI), Spokane, WA, USA, 2022, pp. 510-515.
- [4] H. Bishnoi, A. C. Baisden, P. Mattavelli and D. Boroyevich, "Analysis of EMI Terminal Modeling of Switched Power Converters," *IEEE Transactions on Power Electronics*, vol. 27, no. 9, pp. 3924-3933, Sept. 2012.
- [5] J. Yao, S. Wang and Z. Luo, "Modeling, Analysis, and Reduction of Radiated EMI Due to the Voltage Across Input and Output Cables in an Automotive Non-Isolated Power Converter," *IEEE Transactions on Power Electronics*, vol. 37, no. 5, pp. 5455-5465, May 2022
- [6] S. Kong et al., "An Investigation of Electromagnetic Radiated Emission and Interference From Multi-Coil Wireless Power Transfer Systems Using Resonant Magnetic Field Coupling," *IEEE Transactions on Microwave Theory and Techniques*, vol. 63, no. 3, pp. 833-846, March 2015.
- [7] C. Wu, H. Kim, S. Penugonda and J. Fan, "Analysis and Modeling of the Common-Mode Conducted EMI From a Wireless Power Transfer System for Mobile Applications," *IEEE Transactions on Electromagnetic Compatibility*, vol. 63, no. 6, pp. 2143-2150, Dec. 2021
- [8] C. Wu, H. Kim, A. Huang, J. Fan, S. Pan and T. Li, "An Investigation of Electromagnetic Radiated Emissions from Wireless Charging System for Mobile Device Using Qi Standard," in 2018 IEEE Symposium on Electromagnetic Compatibility, Signal Integrity and Power Integrity (EMC, SI & PI), Long Beach, CA, USA, 2018, pp. 483-488